International Journal of Solids and Structures 50 (2013) 3562–3569

Contents lists available at SciVerse ScienceDirect

International Journal of Solids and Structures

journal homepage: www.elsevier.com/locate/ijsolstr

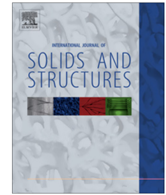

Residual stresses in thin film systems: Effects of lattice mismatch, thermal mismatch and interface dislocations

Alireza Moridi, Haihui Ruan, L.C. Zhang *, Mei Liu

School of Mechanical and Manufacturing Engineering, The University of New South Wales, NSW 2052, Australia

ARTICLE INFO

Article history:
Received 19 September 2012
Received in revised form 20 April 2013
Available online 2 July 2013

Keywords:
Residual stress
Thin film
Thermal mismatch
Lattice mismatch
Dislocation
Critical dislocation density
Thickness-dependence

ABSTRACT

This paper explores the mechanisms of the residual stress generation in thin film systems with large lattice mismatch strain, aiming to underpin the key mechanism for the observed variation of residual stress with the film thickness. Thermal mismatch, lattice mismatch and interface misfit dislocations caused by the disparity of the material layers were investigated in detail. The study revealed that the thickness-dependence of the residual stresses found in experiments cannot be elucidated by thermal mismatch, lattice mismatch, or their coupled effect. Instead, the interface misfit dislocations play the key role, leading to the variation of residual stresses in the films of thickness ranging from 100 nm to 500 nm. The agreement between the theoretical analysis and experimental results indicates that the effect of misfit dislocation is far-reaching and that the elastic analysis of dislocation, resolved by the finite element method, is sensible in predicting the residual stress distribution. It was quantitatively confirmed that dislocation density has a significant effect on the overall film stresses, but dislocation distribution has a negligible influence. Since the lattice mismatch strain varies with temperature, it was finally confirmed that the critical dislocation density that leads to the measured residual stress variation with film thickness should be determined from the lattice mismatch strain at the deposition temperature.

© 2013 Elsevier Ltd. All rights reserved.

1. Introduction

Driven by the increasing demand for faster microprocessors and packing more transistors on a single chip, silicon-on-insulator (SOI) systems have been found a technology to extend the Moore's law in the coming decades (Celler and Cristoloveanu, 2003). However, due to the difference in thermal and mechanical properties of silicon and insulating substrate, residual stresses in vapor deposited layers, by either physical or chemical methods, are inevitable. Such stresses could induce crystallographic defects, leading to higher resistance to the transportation of carriers or phonons, or macroscopic defects, such as buckling, cracking, and delamination, leading to the failure. Hence, understanding the origin of the residual stress variations in such systems is essential.

There are two primary causes of residual stresses in an SOI thin film system. The first is thermal mismatch. When a system is cooled down from a deposition temperature to room temperature, the mismatch of the coefficients of thermal expansion (CTE) of the thin film and the substrate leads to residual stresses in the system. The second cause is the dissimilar lattice structures of the materials, which leads to residual stresses and lattice defects.

Some theoretical and experimental methods have been proposed in the literature to calculate the residual stresses induced by lattice and thermal mismatches and to investigate the stress release by dislocations. Experimentally, these include the methods with the aid of beam curvature (Dumin, 1965), Raman (Englert et al., 1980; Wang et al., 2005) spectroscopy and X-ray diffraction (Liu et al., 2010; Vreeland and Paine, 1986). However, the total residual stresses measured by the experimental methods cannot distinguish the contributions by the mismatches of CTE and lattice structures as well as by the relaxation due to lattice defects.

After the first analytical model developed by Stoney in the early 1900s (Stoney, 1909), a great number of theoretical studies have been conducted, trying to improve the Stoney's equation for calculating the residual stresses in a thin film system. For instance, Timoshenko (1925), Rich (1934) and Klein (2000) relaxed the assumption of negligible film thickness. Freund (2000) considered the effect of finite strain and rotation. Freund and Suresh (2003) removed the assumption of a uniform stress distribution in a thin film. Hu and Huang (2004) investigated the elastic and elastoplastic multilayer thin film systems, and Huang and Rosakis (2005) further extended the Stoney's formula to be applicable to a non-uniform temperature distribution in a thin film substrate system.

Many analytical solutions have also been proposed for calculating the stresses due to misfit dislocations. Vandermerwe (1950) solved the stresses, atomic displacement and energies due

* Corresponding author.
E-mail address: liangchi.zhang@unsw.edu.au (L.C. Zhang).

0020-7683/$ - see front matter © 2013 Elsevier Ltd. All rights reserved.
http://dx.doi.org/10.1016/j.ijsolstr.2013.06.022

to a single misfit dislocation on the interface of two crystals of different lattice spacing. Further developments have afterwards been made to calculate distributions of elastic strains and internal stresses in thin epitaxial films deposited on dissimilar substrates (Ball, 1970; Ball and Van der Merve, 1970; Bonnet, 1996; Jesser and Matthews, 1967, 1968a,b; Matthews, 1968; Matthews and Crawford, 1970; Nakahara, 1989; van der Merwe, 1964; Yao et al., 1999). Gutkin and Romanov (Gutkin et al., 1993; Gutkin and Romanov, 1991, 1992a,b) considered the effects of dislocation interactions, free surface and far field stresses, which were neglected in previous theories and presented a continuum mechanics solution for the stress field around a straight edge dislocation in the interface of two heteroepitaxial materials, applicable directly to a film-on-substrate system. Such analytical models are often complicated in mathematical formulation.

Making use of the stress or strain field surrounding dislocations, the thickness-dependent lattice relaxation was considered (Ayers, 2007). Matthews and Blakeslee (1974) considered the force equilibrium of a threading dislocation and resulted in that the lattice relaxation was inversely proportional to the film thickness. Matthews et al. (1970) included the Peierls force (lattice friction force) in the model and resulted in the kinetic relaxation of lattice strain. Dodson and Tsao (1987) later included the effect of dislocation multiplication and resulted in a more empirical model. All these models, however, were on small lattice mismatch strain (less than 1%), which makes the assumption of small deformation valid and the analytical treatments possible. For the epitaxial thin film system of relatively large mismatch strains, including the silicon-on-sapphire (SOS) system to be considered in the present work, the thickness-dependent lattice relaxation has not been explored. This could be due to the difficulty when the strain is large and when the change of growth mode from layer-by-layer growth to island growth comes into play. It was also noted that for the large mismatch strain in the SOS system, the critical film thickness (at which the first misfit dislocation nucleates) is much less than 10 nanometres according to the theory (cf. e.g., "Heteroepitaxy of Semiconductors" by Ayers). In this case, the film actually grows through domain epitaxy (cf. e.g., Narayan and Larson, 2003; Bayati et al., 2012) and island coalescence (cf. e.g., Hamarthibault and Trilhe, 1981). The misfit dislocations form spontaneously inside islands or during island coalescence (cf. e.g., Legoues et al., 1994; Qian et al., 1997). The classical models based on kinetics of dislocations may not be necessary. Instead, one may directly model the misfit dislocations at the interface and study their influence through elastic analysis of dislocations.

Owing to the fast increase of computational capacity, the finite element (FE) method has become an efficient tool to study the residual stresses attributed to the combined effects of CTE and lattice mismatches as well as the relaxation due to lattice defects. A number of studies have been carried out using the FE method to understand the residual stresses in film-on-substrate systems due to CTE mismatch (Gu and Phelan, 1998; Han et al., 2009; Wright et al., 1994). The focus of these studies was on the effect of deposition temperature, but the simulations were based on two dimensional (2D) models considering only isotropic temperature-independent material properties. A more comprehensive investigation was conducted by Pramanik and Zhang (2011) who carried out a three dimensional (3D) finite element analysis of the thin film residual stresses. In their study, however, the effects of lattice mismatch and dislocations were not included. In our previous study (Liu et al., 2012), it was experimentally found that the residual stress in the silicon film for a silicon-on-sapphire system depends on the film thickness even when the film thickness was of hundreds of nanometres. This result cannot be explained by merely the CTE mismatch. Therefore, a more thorough study is necessary to clarify the origin of residual stress in the thin film.

The aim of this paper is to make a major step forward to reveal the origin of residual stress variation in film-substrate systems when thermal and lattice mismatches and multiple lattice defects come into play all together. To explore the effect of the individuals, and hence to uncover the variation mechanisms of the residual stresses, the contributions of CTE and lattice mismatches and misfit dislocations will be investigated step-by-step.

2. FE modeling

Among the various insulating materials practiced by the semiconductor industry, we consider sapphire in this study. This is because sapphire has recently won a broad acceptance in commercial applications due to its low power consumption and efficient insulating properties. In the silicon-on-sapphire (SOS) technology, a thin hetero-epitaxial silicon layer grows on sapphire at a high temperature. A mono-crystalline sapphire structure has been shown in Fig. 1. To minimize the effect of lattice mismatch between silicon and sapphire, the (100) silicon layer is normally deposited on to the $(1\bar{1}02)$ plane (R-plane) of sapphire (Nakamura et al., 2004). The silicon properties are considered to be orthotropic, whereas the sapphire is regarded as an anisotropic material whose stiffness matrix (Goto et al., 1989) can be converted to the coordinate system indicated in Fig. 1 (i.e., the *x*, *y*, *z* axes are respectively $[\bar{1}101]$, $[11\bar{2}0]$ and $[1\bar{1}02]$). The thermal and mechanical properties of silicon and sapphire are listed in Appendix A.

A schematic of the 3D FE model for investigating the residual stresses in an SOS system is shown in Fig. 2. The model shape resembles an SOS wafer to include all the possible geometrical effects (Moridi et al., 2011). A volume of interest (VOI) is defined in the centre of the model with the finest mesh as shown in Fig. 2. To avoid the boundary effect, the radial dimension of the model was 30 times the thickness of the thin film. Overall, the VOI contained 4440 elements, and the whole model consisted of 34,628 elements. A mesh sensitivity test confirmed that this mesh density was sufficient. The finite element model was solved by ANSYS V12.1 with the 10-noded SOLID 98 elements which can cope with both thermal and mechanical responses.

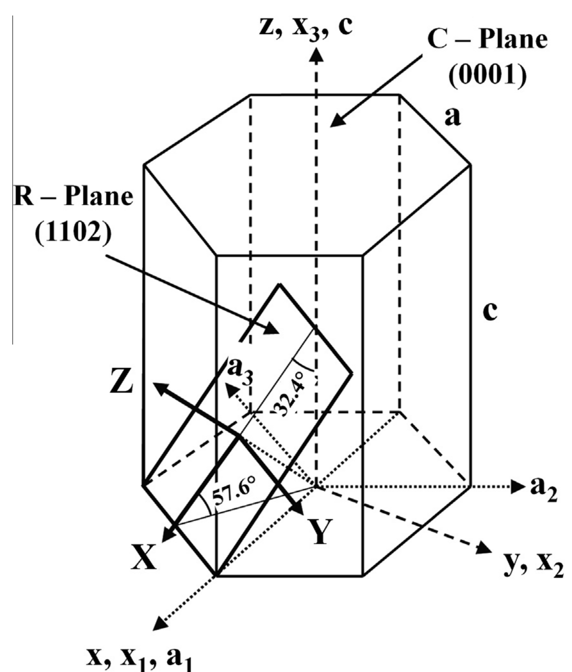

Fig. 1. Coordinate systems in the sapphire crystal and in the $(1\bar{1}02)$ plane.

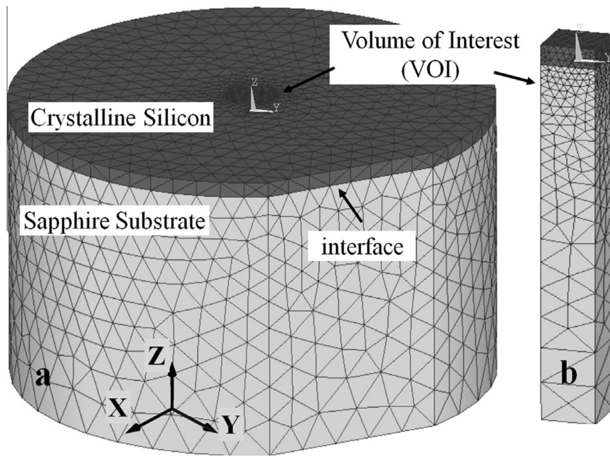

Fig. 2. Geometry of an SOS thin film system: (a) full model (b) VOI.

To simulate the effect of CTE mismatch, the model was cooled down from 900 °C to 25 °C by convection from all the surrounding surfaces with the film coefficient of convection of 10.45 W/m^2 °C (Vodenitcharova et al., 2007). The bottom of the model was fixed in *z*-direction and a node at a bottom corner of the model was fixed in *x*-, *y*- and *z*-axes to eliminate the rigid body motion. The steady-state simulation was separated into 100 sub-steps for resolving the influence of temperature-dependent properties.

To calculate the stresses induced by lattice mismatch, a virtual cooling process was introduced to incur the lattice misfit strains ($\Delta\varepsilon_{xx}$ = 5.9% and $\Delta\varepsilon_{yy}$ = 14.1% at room temperature along sapphire [$\bar{1}101$] and [$11\bar{2}0$] directions, respectively). In this case, the coefficients of thermal expansion of the film are $\alpha_{fx(y)} = \Delta\varepsilon_{x(y)}/\Delta T$, where ΔT is the virtual temperature change, the subscript "*f*" pertains to the film and "*x*" and "*y*" designate sapphire [$\bar{1}101$] and [$11\bar{2}0$] directions respectively.

3. Results and discussion

3.1. Effects of thermal and lattice mismatches

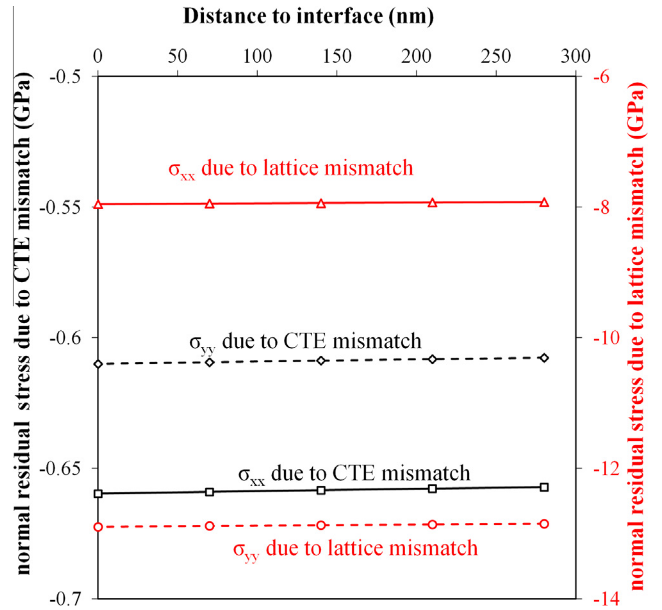

Fig. 3. FE simulation results of stress distribution due to thermal and lattice mismatch.

Fig. 3 shows the in-plane normal residual stresses σ_{xx} and σ_{yy} resulted from thermal and lattice mismatches in a 280 nm thick film. Both σ_{xx} and σ_{yy} are compressive inside the thin film and tensile in the sapphire substrate. σ_{zz} is negligible in comparison with the in-plane normal stresses σ_{xx} and σ_{yy}, which is consistent with experimental findings (Liu et al., 2010) and theoretical calculations (Stoney, 1909). It is interesting to note that the residual stresses do not vary with the depth.

The average in-plane residual stresses σ_{xx} and σ_{yy} for a thin film of 280 nm thickness are −658 MPa and −609 MPa, respectively, due to thermal mismatch, and −7938 MPa and −12,872 MPa, respectively, owing to lattice mismatch, as shown in Fig. 3. The difference between σ_{xx} and σ_{yy} is owing to the anisotropy of sapphire. The calculated thermal and lattice mismatch stresses show that the stress gradient in the thin film is negligible. This is because of the zero shear stress at the centre of the interface. The significant shear stress only occurs near the boundary, which causes the gradient of normal residual stresses in the thin film near the boundary, and may lead to shear failure (Kitamura et al., 2003; Wiklund et al., 1999). At the centre, the shear stresses vanish, which brings about the negligible gradients of the normal residual stresses.

It can be seen that the residual stresses are independent of film thicknesses in the range of 0.280–5 µm. This independency can be rationalized by expressing the residual stresses in non-dimensional form. Invoking the Buckingham's Pi (Π) Theorem (Chen et al., 2009; Fleck et al., 1992; Sun et al., 2000; Wang et al., 2011) and constructing the non-dimensional groups for the three fundamental variables of length, mass, and temperature, the non-dimensional form is obtained:

$$\frac{\sigma_f}{E_f} = f\left(\frac{E_s}{E_f}, \nu_s, \nu_f, \frac{t_s}{t_f}, \Delta\varepsilon\right) \tag{1}$$

where *E*, *ν*, *t* are elastic modulus, poisons ratio and thickness, respectively, the subscripts *s* and *f* pertain to substrate and film thicknesses respectively, and $\Delta\varepsilon$ is the misfit strain. Eq. (1) clearly indicates that the residual stress only depends on ratio t_s/t_f providing that other thermo-mechanical properties are constants. The variation of the non-dimensional residual stresses with the thickness ratio t_s/t_f is shown in Fig. 4. It is noted that if $t_s/t_f \geqslant 20$, the curve levels off. Using the same method, it could be observed that the residual stresses due to lattice mismatch are constant for various film thicknesses if t_s/t_f is larger than 20, as shown in Fig. 4. In most SOS system, t_s/t_f is larger than 100. Therefore the above calculation considering lattice and thermal mismatches shows that the residual stress in the silicon film is independent of film thickness.

In summary, the above analysis indicates that lattice and thermal mismatches are not the cause of residual stress variation with film thickness. Lattice defects must be incorporated into the analysis to understand the thickness-dependent residual stress unambiguously observed in experiments (Liu et al., 2011).

3.2. Effect of interface dislocation

3.2.1. Treatment of interface misfit dislocations

Lattice defects mitigate the residual stress by invoking localized deformation field. Misfit dislocations at interface are the most effective defects in accommodating the mismatch strains (Hull and Bean, 1992). In the present FE model, the effect of edge dislocation was treated by feeding the strain to the elements where an extra plane of atoms is added (Subramaniam and Ramakrishnan, 2003), as shown in Fig. 5. The element size near the interface was taken to be the same as the substrate lattice constants. The burgers vector ***b*** is equal to the spacing a_s of sapphire ($\bar{1}\,1\,0\,1$) or

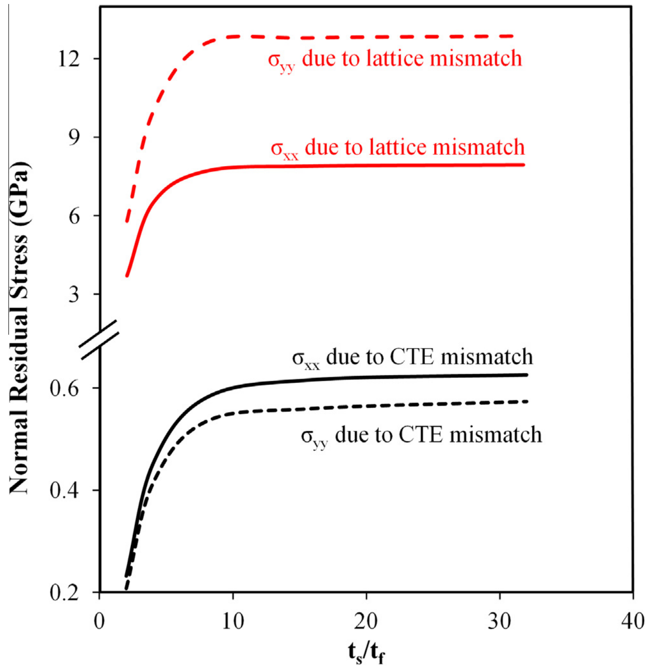

Fig. 4. Effect of $\frac{t_s}{t_f}$ on normal residual stress.

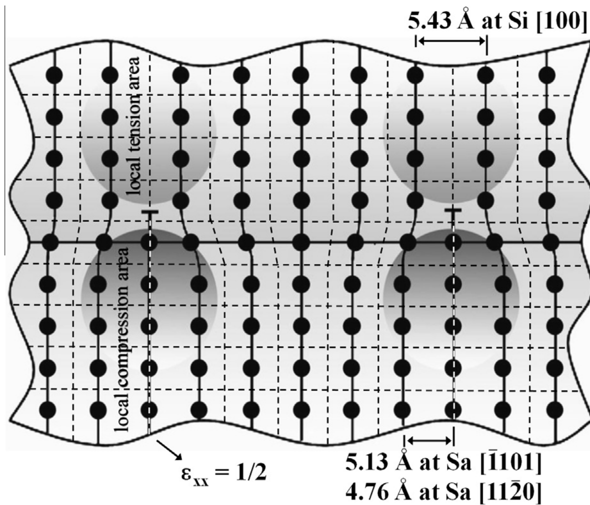

Fig. 5. Schematic of an edge dislocation at the interface.

$(11\bar{2}0)$ planes and in the direction parallel to the interface. The local strain component ε_{xx} corresponding to an edge dislocation is:

$$\varepsilon_{xx} = b/2a_s = 1/2 \tag{2}$$

Therefore, the introduction of dislocations will cause local tension in the film but compression in the substrate, as indicated in Fig. 5.

The stress field around an edge dislocation in the interface of two dissimilar elastic solids has been analytical solved by Gutkin and Romanov (1992a), which is given by:

$$\sigma_{ij}^{d}(x,y) = \sigma_{ij}^{0}(x,y) + \int_{-\infty}^{+\infty} e^{isy} \sum_{\substack{m=1,2 \\ n=x,y}} \Phi^{mn}(s)\hat{\sigma}_{ij}^{mn}(x,s)ds \tag{3}$$

where the first term is the stress field around the dislocation being analyzed and the second term is to account for the effect of far field dislocations. $\Phi^{mn}(s)$ are Fourier transforms of the distributions of the far field dislocations and $\hat{\sigma}_{ij}^{mn}(x,s)$ are the stress fields due to far field dislocations (see (Gutkin and Romanov, 1991, 1992a) for more explanation). Fig. 6 demonstrates the comparison between the analytical and FE results for the uniformly distributed edge dislocation in an isotropic thin film material. It can be seen that although there is a very small discrepancy between the two solutions in the vicinity of the interface, the overall agreement is very good.

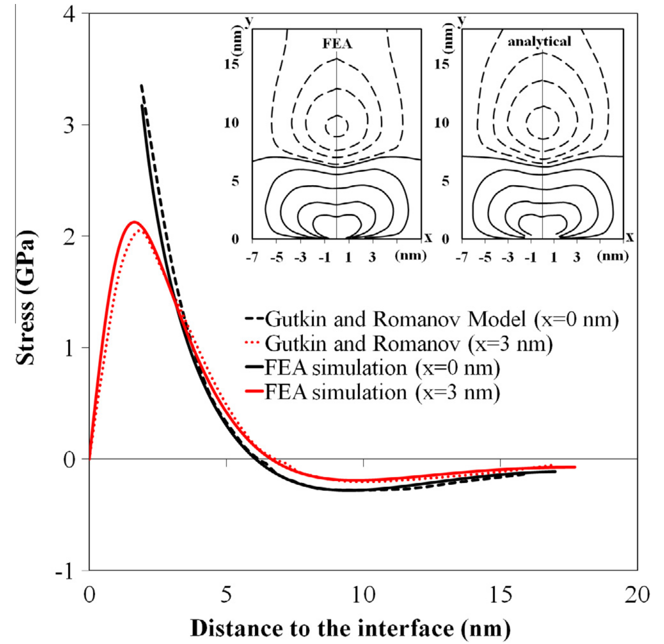

Fig. 6. A comparison between Gutkin and Romanov analytical model and FEA results.

It should be noted that only the 2D plane-strain FE model can be established to investigate the misfit dislocation in a particular atomic plane (e.g., Silicon (100), (010) and (110)) since the 3D model is too demanding and the interaction of two perpendicular misfit dislocations is difficult to be verified. In this plane-strain case, the effect of misfit dislocation on the residual stress may be overestimated due to the additional constrain exerted by the plane-strain condition. For the uniaxial tension under the plane-strain condition, the tensile stress is about 10% larger than that without the constraint. It is therefore expected that the 2D FE model of dislocation also lead to maximum 10% overestimation.

3.2.2. Critical spacing in multiple dislocation system

Having multiple dislocations, the density of dislocations is critical in relaxing the stress due to thermal and lattice mismatches. In order to obtain the critical dislocation density we calculated the strain energy density of the thin film system vs the dislocation spacing in terms of number of lattices between two dislocations n using the FE method. Therefore, the particular dislocation density minimizing the strain energy density of the system should most likely be formed during the material growth and subsequent cooling, which could be called the critical dislocation spacing n_c. However, since the lattice constants and other material properties change with temperature, the critical dislocation spacing may vary. The calculated variation of strain energy density with dislocation spacing is shown in Fig. 7, which gave rise to $n_c = 18$ and 17.8 in the sapphire $[\bar{1}101]$ direction for room and deposition temperatures (25 °C and 900 °C) respectively and 7.1 and 7.25 in the sapphire $[11\bar{2}0]$ direction.

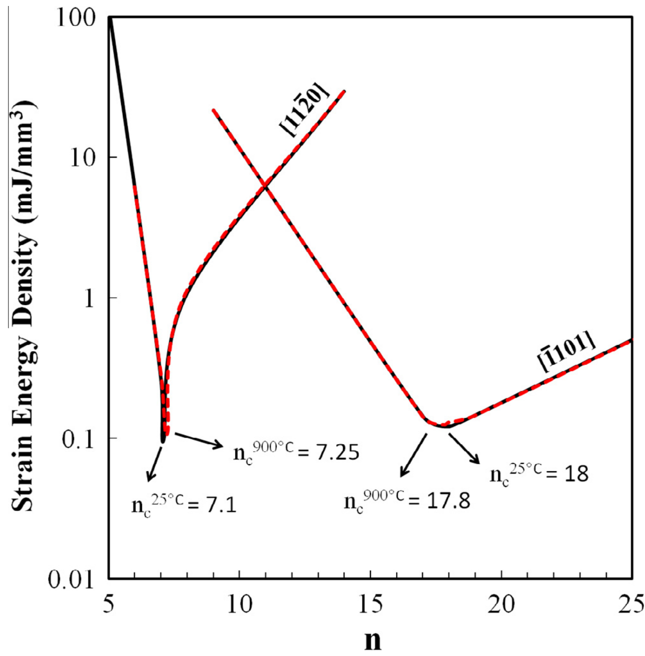

Fig. 7. Strain energy density of the system at room and deposition temperature for different dislocation densities at [$\bar{1}$101] direction and [11$\bar{2}$0] direction.

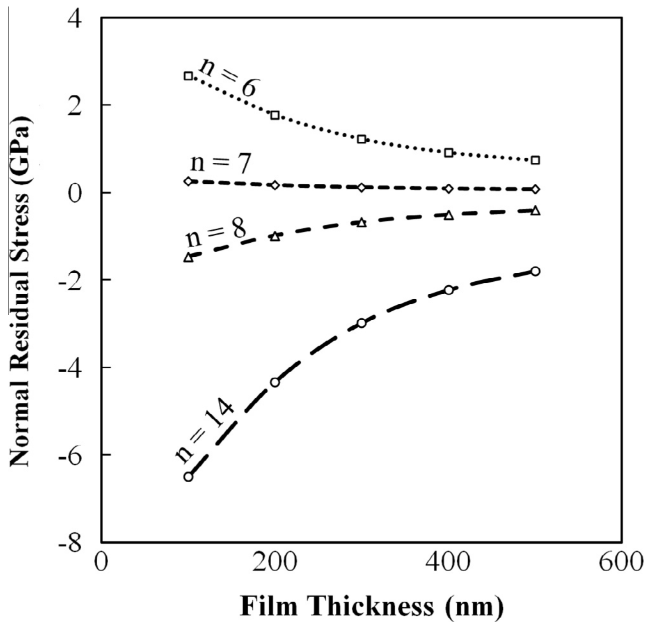

Fig. 8. Effect of dislocation density on the SOS system at [11$\bar{2}$0] direction.

3.2.3. Effects of dislocation density and distribution

The interface dislocation density, which is inversely proportional to *n*, significantly affects residual stresses. To study the sensitivity of residual stresses to *n*, the average dislocation spacing *n* in the present numerical model was varied. Fig. 8 demonstrates the residual stress vs film thickness for different *n* in Si[100] and [010] planes, respectively. It can be seen that dislocations significantly reduce the compressive residual stresses caused by lattice mismatch in the thin film, that the residual stress can change from compressive to tensile in the thin film if the dislocation density is too large, and that a slight change in the density of dislocations, say from 6 to 7 lattice constants between dislocations, can bring about a remarkable change of the residual stresses in the thin film. This great dependency allow us to identify the critical dislocation spacing that lead to the experimental results of thickness-dependent residual stresses and compare it with experimental observation through a high-resolution transmission electron microscopy (HRTEM).

Table 1
Various dislocation distribution cases.

	L_1	L_2	L_3	L_4	L_5	L_6	L_7	L_8	L_9
Case 0	18	18	18	18	18	18	18	18	18
Case 1	18	19	17	18	17	20	17	19	17
Case 2	18	17	20	17	14	22	18	17	19
Case 3	18	19	15	20	15	21	17	19	18

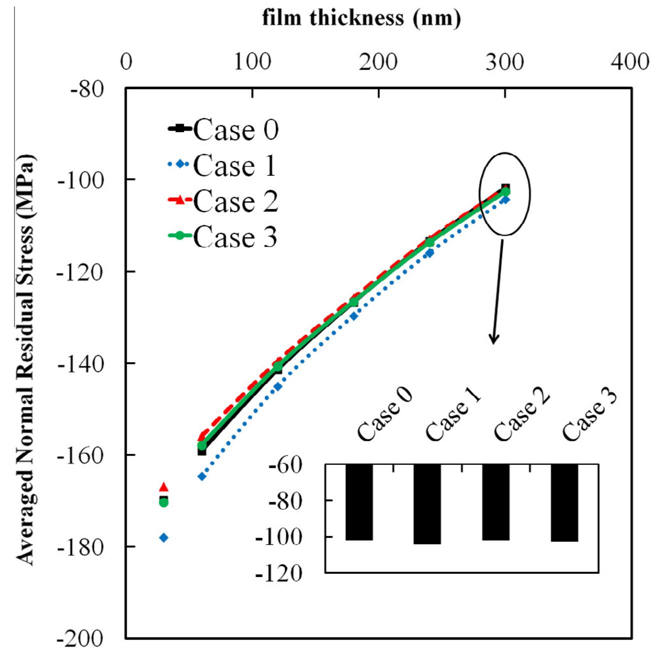

Fig. 9. Effect of dislocation distribution on stress levels of the system.

Since the distribution of dislocations is not necessarily uniform, it is worthwhile to study the effect of dislocation distribution. The effect of three different distributions (280 nm film thickness) with the random spacing of dislocations (generated by Gaussian random number generator), as shown in Table 1, is investigated, where *L* is the number of lattice constants between two adjacent dislocations. As shown in Fig. 9, different distributions of dislocations do not significantly change the residual stress of the system. Although the average stress near the interface is slightly affected by the distribution of dislocations, the stresses at 100 nm far from the interface converge to the value very close to that of the uniform distribution. The inset in Fig. 9 shows the average residual stress due to dislocations throughout the film thickness. This result indicates that the effect of dislocation distribution is insignificant.

3.3. Coupled effect

The calculated residual stresses due to thermal misfit, lattice misfit and dislocations are superposed to have a complete description of the thickness-dependent residual stress in the thin silicon film. Fig. 10 plots the variation of the measured residual stresses with film thickness as well as the results from finite element simulations. It is noted that the residual stresses in a thinner film are

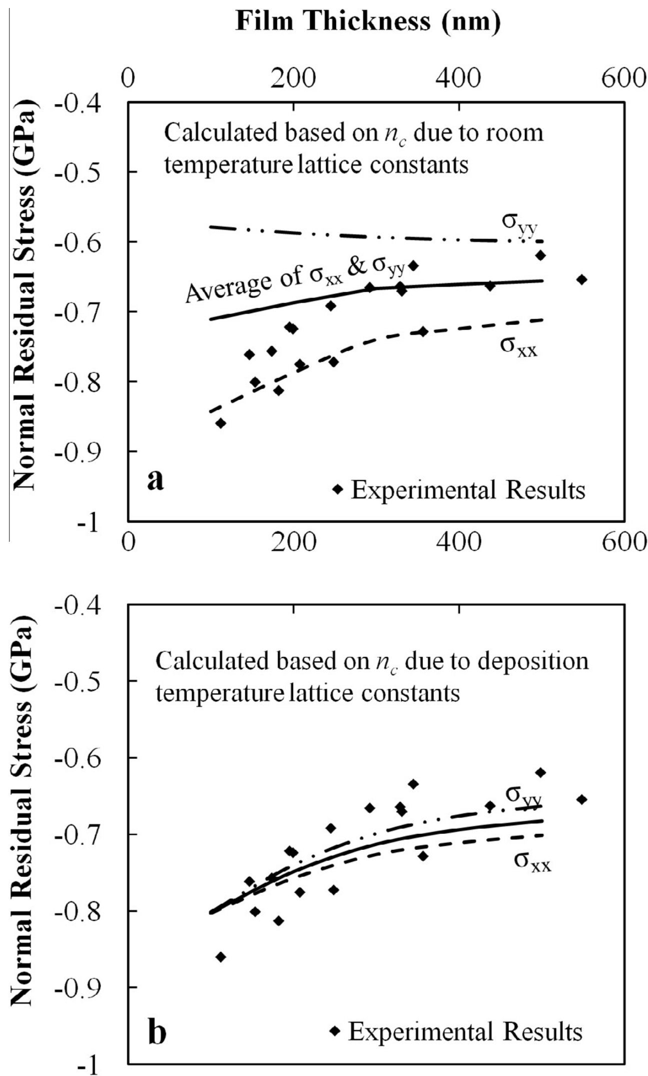

Fig. 10. A comparison between FEA and experimental results based on the minimum energy due to (a) room temperature and (b) deposition temperature lattice constant.

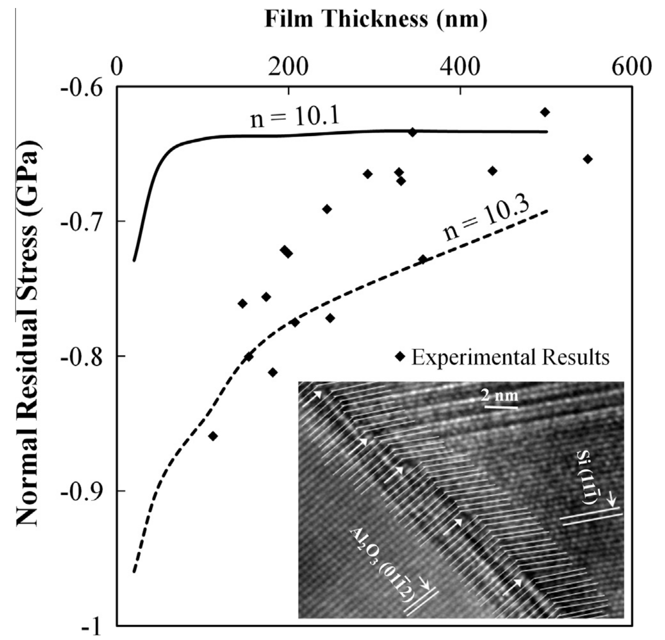

Fig. 11. The calculated residual distributions for n = 10.1 and 10.3.

Table A1
Orthotropic elastic modulus (MPa).

Temperature (°C)	Stiffness matrix (C_{ij} = elastic constants)					
25	1.65E5	63900	63900	0	0	0
	63900	1.65E5	63900	0	0	0
	63900	63900	1.65E5	0	0	0
	0	0	0	79500	0	0
	0	0	0	0	79500	0
	0	0	0	0	0	79500
300	1.61E5	62200	62200	0	0	0
	62200	1.61E5	62200	0	0	0
	62200	62200	1.61E5	0	0	0
	0	0	0	77700	0	0
	0	0	0	0	77700	0
	0	0	0	0	0	77700
600	1.56E5	60300	60300	0	0	0
	60300	1.56E5	60300	0	0	0
	60300	60300	1.56E5	0	0	0
	0	0	0	75700	0	0
	0	0	0	0	75700	0
	0	0	0	0	0	75700
900	1.51E5	58400	58400	0	0	0
	58400	1.51E5	58400	0	0	0
	58400	58400	1.51E5	0	0	0
	0	0	0	73700	0	0
	0	0	0	0	73700	0
	0	0	0	0	0	73700

much larger than those in a thicker film due to the effects of lattice defect. In experiment, chemical etching is employed to reduce the thickness of the silicon film. The Micro-Raman Spectroscopy (Renishaw Invia unit equipped with backscattering configuration), with a spatial resolution of ~10 µm, was employed to measure the local equi-biaxial stress based on the shift of the silicon peak and the local film thickness based on the intensity ratio between silicon peak and the sapphire. A standard setup of 514 nm Argon ion laser and 1800 l/mm grating were utilized to detect the silicon band at around 520 cm^{-1} and the sapphire band at 417 cm^{-1} with the lateral resolution of several microns peak (Liu et al., 2012). The equi-biaxial stress was calculated from the shift of Raman band $\Delta\omega$ (cm^{-1}), i.e., $\sigma = -249\Delta\omega$ (MPa) in case of silicon (Englert et al., 1980). The equi-biaxial state was confirmed by XRD residual stress measurement, which gave the full stress tensor (Liu et al., 2011).

Involving the effects of the thermal and lattice mismatches and the edge dislocations, the present finite element simulations result in the similar thickness dependence to the experimental findings. Since the lattice constants vary with temperature, the critical dislocation spacing that minimizes the strain energy density varies from the deposition temperature to room temperature. It is noted that the critical dislocation spacing (n_c = 17.8 along [$\bar{1}$101] and 7.8 along [11$\bar{2}$0]) at the deposition temperature (900 °C) leads to the consistency with the experimental results. Therefore, we are prone to the assertion that the dislocation structure formed at the deposition process does not vary in the subsequent cooling. Although lattice mismatch in sapphire [11$\bar{2}$0] is more significant than that in [$\bar{1}$101], the higher density of dislocations in [11$\bar{2}$0] cause more relaxation of stress in that direction. It is noted that the calculated residual stresses at two different directions based on the critical dislocation spacing all agrees with the experimental result very

Table A2
Specific heat, thermal conductivity and coefficient of thermal expansion (CTE).

Temperature (°C)	Specific heat (J/g °C)	Thermal conductivity (W/m °C)	Coefficient of thermal expansion (10E−6/°C)
25	0.710	156.9	2.55
300	0.844	68.3	3.78
600	0.895	37.88	4.16
900	0.945	26.54	4.37

well, as shown in Fig. 10, explaining why the residual stresses in the silicon film are almost equi-biaxial (Liu et al., 2011) even through the lattice mismatch strains differ significantly along the two orthogonal directions.

The present model can be further extended to account for the thermal and lattice mismatches in the Si(1 1 0) plane. This is because the high-resolution transmission electron microscope (HRTEM) images that clearly reveal the misfit dislocations can only be obtained for this plane (Liu et al., 2012). Since the interface structure forms at the deposition temperature, we use the lattice constants at the corresponding temperature ($a_f = 3.854$ Å and $a_s = 3.507$ Å) to calculate the critical dislocation spacing based on energy minimization, which gives $n_c = 10.1$, close to the experimentally measured value of 10.3 ± 0.5. In experiment, the dislocation spacing was measured from different HRTEM images. One of them is shown in the inset of Fig. 11. The calculated residual distributions for $n = 10.1$ and 10.3 are both shown in Fig. 11. It is noted that the distribution resulted from $n = 10.3$ is more consistent with the experimental data.

4. Conclusions

The investigation in this paper has presented a comprehensive picture of the influence of thermal and lattice mismatches and misfit dislocations on the residual stress distribution in thin film substrate systems. This study has led to the following conclusions:

Table A4
Specific heat, thermal conductivity.

Temperature (°C)	Specific heat (J/g °C)	Thermal conductivity (W/m °C)
25	0.75	46
300	1.06	18
600	1.19	11
900	1.26	9.6

Table A5
Coefficient of thermal expansion (CTE).

Temperature (°C)	Coefficient of thermal expansion (10E−6/°C)		
	x	y	z
27	5.705	5.147	5.372
77	6.376	5.824	6.046
127	6.904	6.361	6.58
227	7.666	7.131	7.347
327	8.184	7.641	7.859
427	8.568	8.008	8.233
527	8.882	8.298	8.533
627	9.157	8.545	8.791
727	9.407	8.766	9.024
927	9.852	9.155	9.436

(1) Thermal and lattice mismatches do not lead to thickness-dependence of residual stress but interface misfit dislocations do.
(2) The density of interface misfit dislocations significantly affects the overall film residual stresses. However, the distribution of dislocations, which could be random, have a negligible influence on the average residual stress in a thin film system. It is the density of interface misfit dislocations that brings about the residual stress variation with film thickness.
(3) The critical dislocation spacing is determined by the principle of minimal elastic strain energy. The critical spacing thus determined is consistent with direct TEM observations.

Table A3
Anisotropic elastic modulus (MPa).

Temperature (°C)	Stiffness matrix (C_{ij} = elastic constants) in $(1\bar{1}02)$ plane (R-plane)					
22.85	4.7461E5	1.0962E5	1.6107E5	0	0	0
	.0962E5	4.973E5	1.6918E5	0	0	0
	1.6107E5	1.6918E5	4.3345E5	0	0	0
	0	0	0	1.3286E5	0	0
	0	0	0	0	1.8119E5	0
	0	0	0	0	0	1.9187E5
326.85	4.6099E5	1.0633E5	1.6133E5	0	0	0
	1.0962E5	4.86E5	1.6977E5	0	0	0
	1.6133E5	1.6977E5	4.1754E5	0	0	0
	0	0	0	1.2454E5	0	0
	0	0	0	0	1.7611E5	0
	0	0	0	0	0	1.8753E5
626.85	4.4556E5	1.0311E5	1.6062E5	0	0	0
	1.0311E5	4.723E5	1.6889E5	0	0	0
	1.6062E5	1.6889E5	4.007E5	0	0	0
	0	0	0	1.1638E5	0	0
	0	0	0	0	1.6977E5	0
	0	0	0	0	0	1.8222E5
926.85	4.2869E5	0.9927E5	1.5873E5	0	0	0
	0.9927E5	4.573E5	1.6683E5	0	0	0
	1.5873E5	1.6683E5	3.8306E5	0	0	0
	0	0	0	1.084E5	0	0
	0	0	0	0	1.631E5	0
	0	0	0	0	0	1.7653E5

(4) The FE model coupling the effects of thermal mismatch, lattice mismatch and interface dislocations can satisfactorily predict the residual stresses in thin film systems, as firmly supported by the relevant experimental measurements.

Acknowledgement

This research was supported by an ARC grant.

Appendix A

Thin. film (Silicon) material model

Lattice constant in 25 °C: 0.543 nm.
Lattice constant in 900 °C: 0.545 nm (see Tables A1 and A2).

Substrate. (Sapphire) material model

Lattice constant in 25 °C: 0.513 nm at $[\bar{1}101]$ and 0.476 nm at $[11\bar{2}0]$.

Lattice constant in 900 °C: 0.516 nm at $[\bar{1}101]$ and 0.479 nm at $[11\bar{2}0]$ (see Tables A3-A5).

References

Ayers, J.E., 2007. Heteroepitaxy of Semiconductors: Theory, Growth, and Characterization. CRC Press, Boca Raton, FL.
Ball, C.A.B., 1970. Bonding and structure of epitaxial bicrystals. 2. Thin films. Phys. Status Solidi 42, 357–368.
Ball, C.A.B., Van der Merve, J.H., 1970. On bonding and structure of epitaxial bicrystals. 1. Semi-infinite crystals. Phys. Status Solidi 38, 335–344.
Bayati, M.R., Molaei, R., Narayan, R.J., Narayan, J., Zhou, H., Pennycook, S.J., 2012. Domain epitaxy in TiO_2/alpha-Al_2O_3 thin film heterostructures with Ti_2O_3 transient layer. Appl. Phys. Lett. 100, 251606–251609.
Bonnet, R., 1996. Elasticity theory of straight dislocations in a multilayer. Phys. Rev. B 53, 10978–10982.
Celler, G.K., Cristoloveanu, S., 2003. Frontiers of silicon-on-insulator. J. Appl. Phys. 93, 4955–4978.
Chen, Y., Nguyen, T., Zhang, L.C., 2009. Polishing of polycrystalline diamond by the technique of dynamic friction-Part 5: Quantitative analysis of material removal. Int. J. Mach. Tool Manuf. 49, 515–520.
Dodson, B.W., Tsao, J.Y., 1987. Relaxation of strained-layer semiconductor structures by plastic flow. Appl. Phys. Lett. 51, 1325–1327.
Dumin, D.J., 1965. Deformation of and stress in epitaxial silicon films on single-crystal sapphire. J. Appl. Phys. 36, 2700.
Englert, T., Abstreiter, G., Pontcharra, J., 1980. Determination of existing stress in silicon films on sapphire substrate using Raman-spectroscopy. Solid State Electron. 23, 31–33.
Fleck, N.A., Johnson, K.L., Mear, M.E., Zhang, L.C., 1992. Cold-rolling of foil. Proceedings of the Institution of Mechanical Engineers Part B Journal of Engineering Manufacture 206, 119–131.
Freund, L.B., 2000. Substrate curvature due to thin film mismatch strain in the nonlinear deformation range. J. Mech. Phys. Solids 48, 1159–1174.
Freund, L.B., Suresh, S., 2003. Thin Film Materials: Stress, Defect Formation, and Surface Evolution. Cambridge University Press, Cambridge, UK, New York.
Goto, T., Anderson, O.L., Ohno, I., Yamamoto, S., 1989. Elastic-constants of corundum up to 1825-K. J. Geophys. Res. Solid 94, 7588–7602.
Gu, B., Phelan, P.E., 1998. Thermal peeling stress analysis of thin-film high-Tc superconductors. Appl. Supercond. 6, 19–29.
Gutkin, M.Y., Romanov, A.E., 1991. Straight edge dislocation in a thin 2-phase plate. 1. Elastic stress-fields. Phys. Status Solidi A 125, 107–125.
Gutkin, M.Y., Romanov, A.E., 1992a. Misfit dislocations in a thin 2-phase heteroepitaxial plate. Phys. Status Solidi A 129, 117–126.
Gutkin, M.Y., Romanov, A.E., 1992b. Straight edge dislocation in a thin 2-phase plate. 2. Impurity vacancy polarization of plate, interaction of a dislocation with interface and free surfaces. Phys. Status Solidi A 129, 363–377.
Gutkin, M.Y., Kolesnikova, A.L., Romanov, A.E., 1993. Misfit dislocations and other defects in thin-films. Mater. Sci. Eng. A Struct. 164, 433–437.
Hamarthibault, S., Trilhe, J., 1981. Transmission electron observations of the early stage of epitaxial-growth of silicon on sapphire. J. Electrochem. Soc. 128, 581–585.
Han, J.C., Zhou, Y.F., Zhang, Y.M., Yao, W., 2009. Finite element analysis of stress in contacting zone of film and substrate. Surf. Coat Tech. 203, 1665–1669.
Hu, Y.Y., Huang, W.M., 2004. Elastic and elastic–plastic analysis of multilayer thin films: closed-form solutions. J. Appl. Phys. 96, 4154–4160.
Huang, Y., Rosakis, A.J., 2005. Extension of Stoney's formula to non-uniform temperature distributions in thin film/substrate systems. The case of radial symmetry. J. Mech. Phys. Solids 53, 2483–2500.
Hull, R., Bean, J.C., 1992. Misfit dislocations in lattice-mismatched epitaxial-films. Crit. Rev. Solid State 17, 507–546.
Jesser, W.A., Matthews, J.W., 1967. Evidence for pseudomorphic growth of iron on copper. Philos. Mag. 15, 1097–1106.
Jesser, W.A., Matthews, J.W., 1968a. Growth of Fcc cobalt on nickel. Acta Metall. 16, 1307–1311.
Jesser, W.A., Matthews, J.W., 1968b. Pseudomorphic deposits of cobalt on copper. Philos. Mag. 17, 461–473.
Kitamura, T., Hirakata, H., Itsuji, T., 2003. Effect of residual stress on delamination from interface edge between nano-films. Eng. Fract. Mech. 70, 2089–2101.
Klein, C.A., 2000. How accurate are Stoney's equation and recent modifications. J. Appl. Phys. 88, 5487–5489.
Legoues, F.K., Reuter, M.C., Tersoff, J., Hammar, M., Tromp, R.M., 1994. Cyclic growth of strain-relaxed Islands. Phys. Rev. Lett. 73, 300–303.
Liu, M., Zhang, L.C., Brawley, A., Atanackovic, P., Duvall, S., 2010. Determining the complete residual stress tensors in SOS hetero-epitaxial thin film systems by the technique of X-ray diffraction. Adv. Mater. Proc. Ix 443, 742–747.
Liu, M., Ruan, H., Zhang, L., 2011. Investigation of lattice mismatch stress in SOS thin film systems by Raman scattering and XRD techniques, in: AES-ATEMA Milan, Italy.
Liu, M., Ruan, H.H., Zhang, L.C., Moridi, A., 2012. Effects of misfit dislocation and film-thickness on the residual stresses in epitaxial thin film systems: experimental analysis and modelling. J. Mater. Res. 27, 2737–2745.
Matthews, J.W., 1968. Preparation of thick beta-cobalt films. Philos. Mag. 18, 1149–1154.
Matthews, J.W., BlakesleeA, E., 1974. Defects in epitaxial multilayers: I. Misfit dislocations. J. Cryst. Growth 27, 118–125.
Matthews, J.W., Crawford, J.L., 1970. Accommodation of misfit between single-crystal films of nickel and copper. Thin Solid Films 5, 187–198.
Matthews, J.W., Mader, S., Light, T.B., 1970. Accommodation of misfit across the interface between crystals of semiconducting elements or compounds. J. Appl. Phys. 41, 3800–3804.
Moridi, A., Ruan, H.H., Zhang, L.C., Liu, M., 2011. A finite element simulation of residual stresses induced by thermal and lattice mismatch in thin films. In: Haddad, Y.M. (Ed.), Seventh International Conference, on Advances and Trends in Engineering Materials and their Applications, Advanced Engineering Solutions, Milan, p. 57.
Nakahara, S., 1989. Formulations of Vandermerwe misfit dislocation theory using a continuous distribution of infinitesimal interface dislocations. Mater. Sci. Eng. A Struct. 112, 43–48.
Nakamura, T., Matsuhashi, H., Nagamoto, Y., 2004. Silicon on sapphire (SOS) device technology. In: Oki Technical Review, Technologies that Support the e-Society, vol. 71, (200), 4.
Narayan, J., Larson, B.C., 2003. Domain epitaxy: a unified paradigm for thin film growth. J. Appl. Phys. 93, 278–286.
Pramanik, A., Zhang, L.C., 2011. Residual stresses in silicon-on-sapphire thin film systems. Int. J. Solids Struct. 48, 1290–1300.
Qian, W., Skowronski, M., et al., 1997. Dislocation density reduction in GaSb films grown on GaAs substrates by molecular beam epitaxy. J. Electrochem. Soc. 144, 1430–1434.
Rich, T.A., 1934. Thermo-mechanics of bimetals. Gen. Electr. Rev. 37, 102–105.
Stoney, G.G., 1909. The tension of metallic films deposited by electrolysis. P. R. Soc. Lond. A Conta 82, 172–175.
Subramaniam, A., Ramakrishnan, N., 2003. Analysis of thin film growth using finite element method. Surf. Coat Tech. 167, 249–254.
Sun, J., Zhang, L.C., Mai, Y.W., Payor, S., Hogg, M., 2000. Material removal in the optical polishing of hydrophilic polymer materials. J. Mater. Process. Technol. 103, 230–236.
Timoshenko, S., 1925. Analysis of bi-metal thermostats. J. Opt. Soc. Am. Rev. Sci. 11, 233–255.
van der Merwe, J.H., 1964. Interfacial misfit and bonding between oriented films and their substrates. In: Francombe, M.H., Sato, H. (Eds.), Single Crystal Films. Pergamon Press, Oxford, pp. 139–163.
Vandermerwe, J.H., 1950. On the stresses and energies associated with inter-crystalline boundaries. P. Phys. Soc. Lond. A 63, 616–637.
Vodenitcharova, T., Zhang, L.C., Zarudi, I., Yin, Y., Domyo, H., Ho, T., Sato, M., 2007. The effect of anisotropy on the deformation and fracture of sapphire wafers subjected to thermal shocks. J. Mater. Process. Technol. 194, 52–62.
Vreeland, T., Paine, B.M., 1986. X-ray-diffraction characterization of multilayer semiconductor structures. J. Vac. Sci. Technol. A Vac. Surf. Films 4, 3153–3159.
Wang, Q.Y., Wang, J., Wang, J.H., Liu, Z.L., Lin, L.Y., 2005. Characterization of stress induced in SOS and Si/gamma-Al_2O_3/Si heteroepitaxial thin films by Raman spectroscopy. J. Cryst. Growth 280, 222–226.
Wang, J., Moridi, A., Mathew, P., 2011. Micro-grooving on quartz crystals by an abrasive air jet. P. I. Mech. Eng. C J. Mech. 225, 2161–2173.
Wiklund, U., Gunnars, J., Hogmark, S., 1999. Influence of residual stresses on fracture and delamination of thin hard coatings. Wear 232, 262–269.
Wright, J.K., Williamson, R.L., Maggs, K.J., 1994. Finite-element analysis of the effectiveness of interlayers in reducing thermal residual-stresses in diamond films. Mater. Sci. Eng. A Struct. 187, 87–96.
Yao, Y.G., Wang, T.C., Wang, C.Y., 1999. Peierls–Nabarro model of interfacial misfit dislocation: an analytic solution. Phys. Rev. B 59, 8232–8236.